PROCEEDINGS OF SCIENCE

Neutrino imaging of the Galactic Centre and Millisecond Pulsar Population

Paul C. W. Lai,[a,*] **Matteo Agostini,**[b] **Foteini Oikonomou,**[c] **Beatrice Crudele,**[b] **Ellis R. Owen**[d] **and Kinwah Wu**[a]

[a] *Mullard Space Science Laboratory, University College London, Holmbury St. Mary, Surrey RH5 6NT, United Kingdom*

[b] *Department of Physics and Astronomy, University College London, Gower Street, London, WC1E 6BT, United Kingdom*

[c] *Institutt for Fysikk, Norwegian University of Science and Technology, Trondheim, Norway*

[d] *Theoretical Astrophysics, Department of Earth and Space Science, Graduate School of Science, Osaka University, Toyonaka, Osaka 560-0043, Japan*

E-mail: chong.lai.22@ucl.ac.uk

In this work, we consider the possible presence of a large population of millisecond pulsars in the Galactic Centre. Their direct detection would be challenging due to severe pulse broadening caused by scattering of radiation. We propose a new method to constrain their population with neutrino imaging of the Galactic Centre. Millisecond pulsars are proposed cosmic-ray accelerators. The high-energy protons they produce will collide with the baryonic matter in the central molecular zone to create charged and neutral pions that decay into neutrinos and γ-rays, respectively. The specific neutrino and γ-ray fluxes must be below their corresponding observed values, allowing us to put a conservative upper limit on the millisecond pulsar population of $N_{\rm MSP} < 10{,}000$ within a galacto-centric radius of 20 pc. This upper limit is sensitive to the proton acceleration efficiency of the pulsars, but is less dependent on the particle injection spectral index and the choice of mass tracers. The population will be better constrained when high resolution neutrino observations of the Galactic Centre become available. The presence of these millisecond pulsars can account for the γ-ray excess in the Galactic Centre.

38th International Cosmic Ray Conference (ICRC2023)
26 July - 3 August, 2023
Nagoya, Japan

*Speaker

PoS(ICRC2023)1069

1. Overview

It has been suggested that the Galactic Centre (GC) habours a large number of pulsars [see 1, 2]. Verifying their presence or absence will help to resolve issues such as the origin(s) of the multiple components of γ-rays, and the stellar-mass black-hole content in the GC region. The fast rotation and strong magnetic field of a pulsar create a large electric potential which would accelerate charged particles to high energies. There is clear evidence showing pulsars are able to produce high-energy electrons and positrons [e.g. from studies of the Crab Pulsar, 3]. Accelerated high energy protons emit radiation much less strongly than their leptonic counterparts. Evidence for their presence is therefore more challenging to establish, and an unambiguous observational signature of hadronic particles from pulsars is yet to be found. However, the acceleration of hadronic particles in pulsar environments has not been ruled-out, and theoretical studies have considered the possibility that pulsars can accelerate both protons and leptons [e.g. 4–6]. This study therefore also introduces an indirect means to reveal the presence of cosmic-ray (CR) protons accelerated by pulsar populations.

The TeV γ-ray emission observed from the GC region implies the presence of localised PeV accelerators, if the γ-rays are by-products of CR interactions [see 7, 8]. The massive nuclear black hole (Sgr A*), supernova remnants, star clusters and pulsars are candidate PeV charged-particle accelerators. Considering a CR diffusion timescale of $t_{\rm diff} = r^2/(4D) \sim 3 \times 10^5$ yr for $r \sim 200$ pc and $D \sim 10^{28}\,{\rm cm^2\,s^{-1}}$, the $1/r$ spatial distribution of CR density in the Galaxy suggests that Sgr A* must have been active until at least 3×10^5 yr ago, if it were the primary source of CRs [7, 9]. Sgr A* has experienced several outbursts over the past few hundred years [see e.g. 10], however it has spent most of this time in a quiescent state. The energy output of the recent outbursts is not sufficient to account for the abundance of GC CRs. If associated with Sgr A*, the estimated age range of the *Fermi* bubbles indicates that it underwent an active episode 1-10 Myr ago [11, 12]. This episode may also be insufficient to produce the observed Galactic CR distribution. Indeed, H.E.S.S. observations [7] suggest that the injection of PeV CRs at the GC is more likely to be continuous rather than episodic. Extreme supernova remnants could produce PeV CRs [13], but such extreme supernovae are uncommon. The two remaining CR source candidates are therefore nuclear star clusters and pulsars, in particular millisecond pulsars (MSPs) [6, 14]. In this work, we focus on the latter case.

Direct detection of GC MSPs through traditional timing radio observations is difficult. This is because of severe pulse broadening caused by scattering in ionised gas. Alternative means must therefore be sought to detect this pulsar population, if present. We propose that neutrino imaging of the GC will constrain the MSP population more stringently than the use of γ-rays. The recent IceCube detection of the Milky Way neutrino flux has an angular resolution of $\sim 10^\circ$ [15], much larger than the region of interest in this work ($\sim 1^\circ$). The IceCube result therefore cannot be directly compared to the results presented in this study. However, higher-fidelity neutrino observations will be achievable in the near future, and it is timely to discuss the applications of neutrino imaging. Future observations will be able to constrain the GC MSP population, and hence shed light on a number of open questions about the GC region, including its γ-ray excess and the missing pulsar problem [see e.g. 2, 16].

2. Model Scenario

The scenario we consider in this work is summarised as follows. A large number of MSPs reside in the stellar cluster around Sgr A*. Protons accelerated by these MSPs are scattered by the interstellar magnetic field. Co-located with the MSPs in the GC is a spatially extended diffuse baryonic medium, where most of the baryons are locked in the clouds of the central molecular zone (CMZ). The GC CRs interact with the CMZ baryons via p-p collisions. These interactions produce charged and neutral pions which rapidly decay into neutrinos and γ-rays, respectively.

2.1 Millisecond pulsars as particle accelerators

For a MSP with a rotational period P_s and polar strength B for a dipolar magnetic field, the spin-down luminosity is

$$L_\mathrm{sd} = 1.4\times10^{35}\,\mathrm{erg\,s^{-1}}\left(\frac{B}{10^8\,\mathrm{G}}\right)^2\left(\frac{R_\mathrm{ns}}{10\,\mathrm{km}}\right)^6\left(\frac{P_\mathrm{s}}{1\,\mathrm{ms}}\right)^{-4}\,, \tag{1}$$

where R_ns is the MSP (neutron star) radius. The maximum energy can be attained by a proton is

$$E_\mathrm{p,max} = 2\eta\,\mathrm{PeV}\left(\frac{B}{10^8\,\mathrm{G}}\right)\left(\frac{R_\mathrm{ns}}{10\,\mathrm{km}}\right)^2\left(\frac{P_\mathrm{s}}{1\,\mathrm{ms}}\right)^{-1} \tag{2}$$

[6]. The maximum energy depends on the pair production efficiency. The higher the efficiency, the lower the maximum energy. This is parametrised by η, which ranges from 0.25 to 1. As only a fraction of the rotational power of a MSP is available for proton acceleration, a scaling parameter f_p is introduced. This gives the CR power of a MSP:

$$f_\mathrm{p}\,L_\mathrm{sd} = \int_{m_\mathrm{p}c^2}^{\infty}\mathrm{d}E_\mathrm{p}\;Q_\mathrm{psr}(E_\mathrm{p})\,E_\mathrm{p} \propto \int_{m_\mathrm{p}c^2}^{\infty}\mathrm{d}E_\mathrm{p}\;E^{\Gamma+1}e^{-E_\mathrm{p}/E_\mathrm{p,max}}\,, \tag{3}$$

where $Q_\mathrm{psr}(E_\mathrm{p})$ is the spectral power in units of $(\mathrm{erg\,s})^{-1}$, Γ is spectral index of CR protons accelerated by the MSP, and m_p is the proton rest mass. The high-energy spectral cut-off is set by $E_\mathrm{p,max}$ (see Equation 2).

2.2 Cosmic-ray transport with hadronic interactions

We model the distribution of CR protons using the transport equation in the diffusion limit, characterised by an energy-dependent diffusion coefficient, $D(E_\mathrm{p})$:

$$\frac{\partial n_\mathrm{CRp}(E_\mathrm{p},r,t)}{\partial t} - \nabla\cdot\left[D(E_\mathrm{p})\nabla n_\mathrm{CRp}(E_\mathrm{p},r)\right] = Q_\mathrm{psr}(E_\mathrm{p})\,n_\mathrm{MSP}(r) - c\left[n_\mathrm{H}\,\sigma_\mathrm{pp}(E_\mathrm{p})\right]n_\mathrm{CRp}(E_\mathrm{p},r,t)\,, \tag{4}$$

where n_CRp is the CR proton number density, n_H is the Hydrogen number density in the diffuse medium, and n_MSP is the MSP number density in the GC region. The two terms on the right side of the equation are the rates of particle loss (through inelastic hadronic p-p interactions with a cross-section σ_pp) and of production of CR protons by MSPs. The solution to the transport equation is

$$n_\mathrm{CRp}(E_\mathrm{p},r) \approx \frac{Q_\mathrm{psr}(E_\mathrm{p})}{4\pi D(E_\mathrm{p})}\int_r^{\infty}\mathrm{d}r'\;\frac{N_\mathrm{MSP}(r')}{r'^2} \tag{5}$$

in the limits $r \ll 2\sqrt{Dt}$ (stationary limit) and $r \ll \sqrt{D/(cn_{\rm H}\sigma_{\rm pp})}$ (negligible absorption), with the number of pulsars within a radius r' given by $N_{\rm MSP}(r') = \int_0^{r'} {\rm d}r\, n_{\rm MSP}(r)\, 4\pi r^2$. The all-favour neutrino and γ-ray fluxes are given by

$$\frac{{\rm d}N_{\nu/\gamma}}{{\rm d}E_{\nu/\gamma}} = \frac{1}{4\pi d^2} \int {\rm d}V\, \frac{{\rm d}\dot{n}_{\nu/\gamma}(E_{\nu/\gamma})}{{\rm d}E_{\nu/\gamma}} \tag{6}$$

(observed at Earth), where

$$\frac{{\rm d}\dot{n}_{\nu/\gamma}(E_{\nu/\gamma})}{{\rm d}E_{\nu/\gamma}} = c\, n_{\rm H} \int_{m_{\rm p}}^{\infty} \frac{{\rm d}E_{\rm p}}{E_{\rm p}}\, F_{\nu/\gamma}\left(\frac{E_{\nu/\gamma}}{E_{\rm p}}, E_{\rm p}\right) \sigma_{\rm pp}(E_{\rm p})\, n_{\rm CRp}(E_{\rm p}, r)\ . \tag{7}$$

Here, $F_{\nu/\gamma}$ is the spectrum of the secondary neutrinos and γ-rays produced by a single p-p collision. We calculated this using the QGSJET-II-04m hadronic model provided by the `AAfragpy` package [17, 18].

2.3 Central Molecular Zone

The observed neutrino and γ-ray fluxes are linearly dependent on the number density of target baryons (see Equation 7), which are predominantly Hydrogen located in the CMZ. Ideally, we would use a 3D number density profile to capture the distribution of CMZ baryons. However, this is not directly observable. Instead, we adopt a line-of-sight Hydrogen column density, which can be derived from infrared (IR) or radio observations, to compute a map of neutrino and γ-ray intensities. The rationale behind this is that both neutrinos and γ-rays do not suffer significant attenuation when propagating from the GC region to reach the Earth. CS (carbon monosulfide) and dust emission are often used as mass tracers for molecular clouds (MCs), but they give substantially different baryon distribution profiles in the CMZ [cf. 19, 20]. We therefore consider both CS and dust observations, taken from [19] and [20], respectively, to derive Hydrogen column density maps. The region within 359.4° to 0.95° in Galactic longitude and −0.25° to +0.15° in Galactic latitude sufficiently covers the densest structure of CMZ. Integration over this region yields a total gas mass of $\sim 7 \times 10^7\,{\rm M}_\odot$.

3. Results and discussion

We adopt a distance of $d = 8.28\,{\rm kpc}$ from Earth to the GC [23] and a diffusion coefficient $D(E_{\rm p}) = 2.24 \times 10^{28}\ {\rm cm^2\,s^{-1}}\,(E_{\rm p}/1\,{\rm GeV})^{\alpha}$ [24] , where $\alpha = 0.21$ for the transport of CRs near the GC. Two groups of MSPs, with $(B, R_{\rm ns}, P_{\rm s}) = (10^8\,{\rm G}, 10\,{\rm km}, 1\,{\rm ms})$ and $(B, R_{\rm ns}, P_{\rm s}) = (10^{10}\,{\rm G}, 10\,{\rm km}, 10\,{\rm ms})$, are considered in our calculations. These have the same spin-down luminosity but a different maximum accelerated CR proton energy. They are uniformly distributed within a galacto-centric radius of 20 pc. The energy spectral indices of the CR protons that they produce are $\Gamma = -1, -1.5$ and -2.

Figure 1 shows the all-flavour neutrino surface brightness images at $E_\nu = 100\,{\rm TeV}$ for the case with $N_{\rm MSP} = 5 \times 10^3$, $f_{\rm p} = 1\%$, and MSP CR energy spectral index $\Gamma = -1$. In generating the neutrino surface brightness images, we also considered other choices of CR spectral properties. We found that the choices of Γ and E_ν do not alter the presence or absence of the locally peaked emission in the neutrino maps, which correspond to the region with a high concentration of baryons. However, they do change the brightness normalisation, implying there is a degeneracy of the MSP

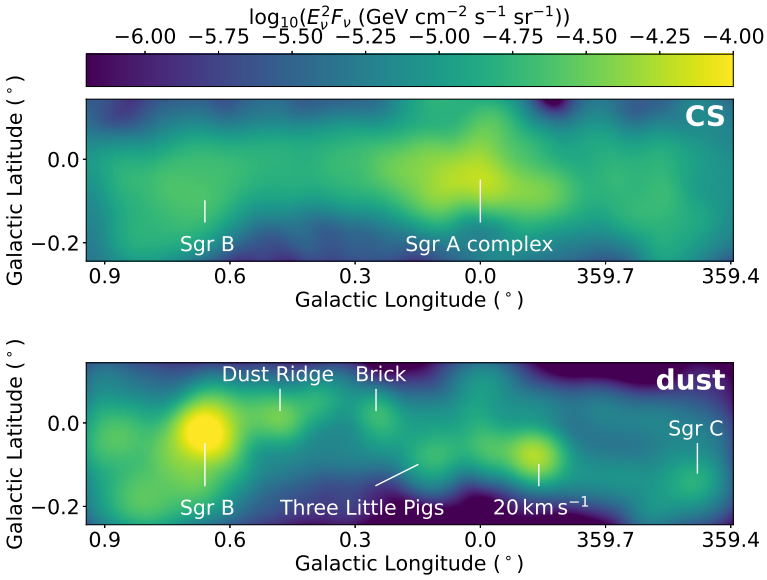

Figure 1: All-flavor neutrino surface brightness images at $E_\nu = 100\,\mathrm{TeV}$ for $\Gamma = -1$, $N_{\mathrm{MSP}} = 5 \times 10^3$ and $f_{\mathrm{p}} = 1\%$. The effective angular resolution is 0.077°, which is the same as the angular resolution of the CS observations [19]. The panels show the results using CS and dust emission as the mass tracer, respectively. Some known MCs are marked, with others listed in Refs. [21, 22].

CR spectra parameters, MSP number density, and the efficiency of converting MSP rotational energy to CR luminosity. The effective angular resolution of the images is 0.077°. Figure 1 indicates that the features shown in the two panels could be resolved at a spatial resolution of about 0.2°, or even 0.3°, which would be achievable with new observatories located in the northern hemisphere, e.g. KM3NeT, Baikal-GVD and P-ONE.

By comparing the two panels in Figure 1 we may draw two qualitative conclusions. First, modelling of the baryon column density derived from CS emission or dust emission gives different features in the neutrino surface brightness map. A direct consequence of this is that CRs in the GC region are baryon “torches", and neutrino imaging can be used as a means to assess the reliability of different mass tracers of MCs in the GC. Second, integrating the surface brightness over the image gives the emission power of neutrinos and, hence, yields a constraint on the power of the CRs that have produced them. This gives us some information about the spectral properties of MSP CRs, specified by Γ and $E_{\mathrm{p,max}}$, the number density of MSPs, and the efficiency with which MSPs can produce CRs (f_{p}). A strong constraint cannot be drawn due to degeneracies between these parameters and the convolution between some of them.

Figure 2 shows the spectra of the total all-flavor neutrino and γ-ray emission from the entire CMZ. The upper panels show how their spectra change with Γ by fixing the normalisation $f_{\mathrm{p}} N_{\mathrm{MSP}}$. We then adjust the population N_{MSP} for different Γ to match H.E.S.S. observations [8], which is shown in the lower panels of Figure 2. The γ-ray flux derived from our models should not exceed the H.E.S.S. observation, which constrains the possible population of MSPs. For $\Gamma = -1$, we obtained a conservative upper limit of $N_{\mathrm{MSP}} < 10{,}000$, assuming that $f_{\mathrm{p}} = 1\%$. In all the models considered, the all-flavour neutrino specific flux tracks the γ-ray specific flux closely. Similar brightness features

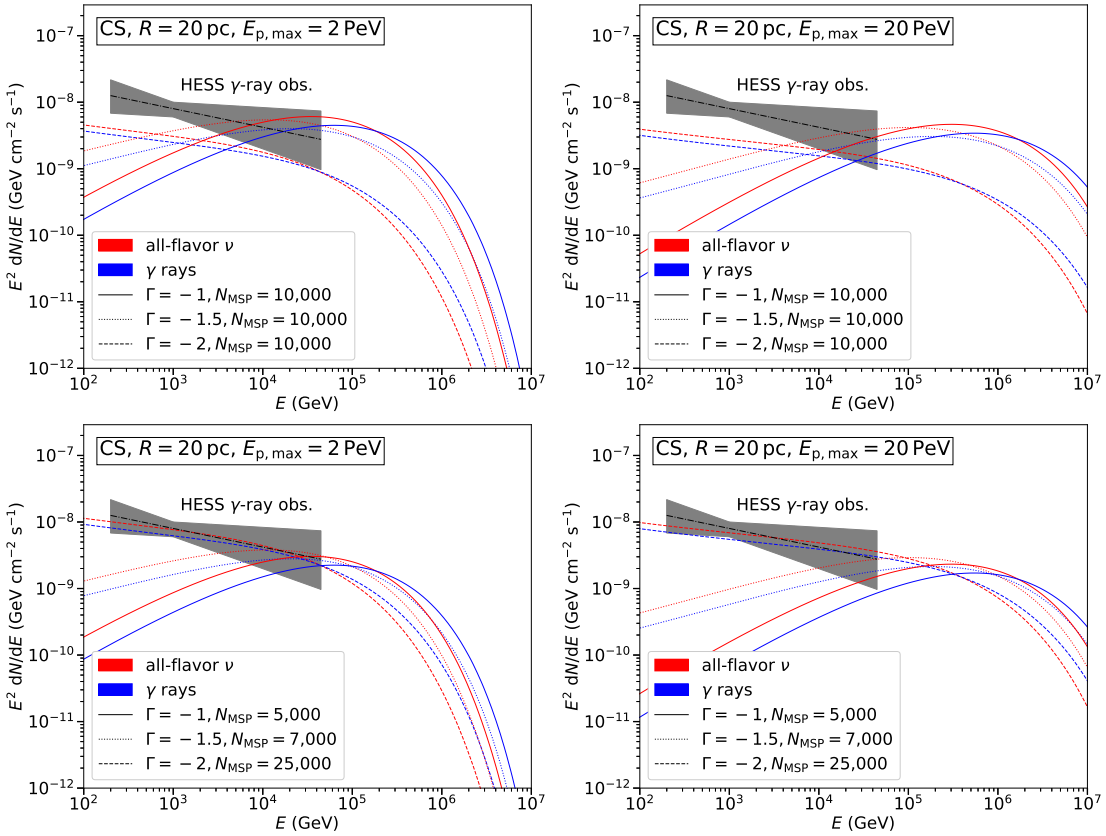

Figure 2: The computed total spectra of all-flavor neutrino and γ-ray emission from the entire CMZ within a galacto-centric radius of $R = 20$ pc, using CS emission as the baryon tracer. The spectrum of the γ-rays from the GC detected by H.E.S.S. [8] is also shown as a dotted dash line, with the uncertainties represented by the grey band. In the upper panels, $N_{\rm MSP}$ is set to be the same for all the models. In the lower panels, the normalisation for $N_{\rm MSP}$ is chosen such that the computed specific γ-ray flux matches that derived from H.E.S.S. observations. The acceleration efficiency $f_{\rm p}$ is set to be 1 per cent for all our calculations.

are therefore expected to be present in the neutrino and γ-ray surface brightness maps if there is no leptonic γ-ray emission. This implies that spectral imaging neutrino observations allow the properties of CR accelerators to be probed, and their population to be constrained (if adopting a specific candidate accelerator, such as GC MSPs).

4. Conclusion

We consider MSPs as particle accelerators whose CRs interact with the baryons in the CMZ of the GC through hadronic processes. We calculate the neutrino and γ-ray emission resulting from these hadronic processes, and show neutrino images of the GC using CS and dust emission as tracers of target baryons in the CMZ. We demonstrate that neutrino imaging could be used to determine the baryon distribution in the GC. We compute the specific fluxes of neutrino and γ-ray emission for the case of CS emission as the baryon tracer, subject to the limits set by H.E.S.S. observations. We obtain a conservative upper limit of $N_{\rm MSP} < 10{,}000$ for the GC MSP population, with a CR energy spectral index $\Gamma = -1$ and efficiency of $f_{\rm p} = 1$ per cent, by converting the rotational power

of pulsars to CR power. This limit varies with the model parameters, and is inversely proportional to f_p. The sizes of MSP populations that we obtain are consistent with those required to account for the GeV γ-ray excess in GC. The results obtained in this work are a benchmark for future neutrino detectors that will observe the GC at high angular resolution ($< 1^\circ$).

Acknowledgments

PCWL is supported by the UCL Graduate Research Scholarship and Overseas Research Scholarship. PCWL, MA, BC and KW are supported by the UCL Cosmoparticle Initiative. ERO is an international research fellow under the Postdoctoral Fellowship of the Japan Society for the Promotion of Science (JSPS), supported by JSPS KAKENHI Grant Number JP22F22327.

References

[1] E. Pfahl and A. Loeb, *Probing the Spacetime around Sagittarius A* with Radio Pulsars*, ApJ **615** (2004) 253 [astro-ph/0309744].

[2] R.S. Wharton, S. Chatterjee, J.M. Cordes, J.S. Deneva and T.J.W. Lazio, *Multiwavelength Constraints on Pulsar Populations in the Galactic Center*, ApJ **753** (2012) 108 [1111.4216].

[3] R. Bühler and R. Blandford, *The surprising Crab pulsar and its nebula: a review*, *Reports on Progress in Physics* **77** (2014) 066901 [1309.7046].

[4] P. Blasi, R.I. Epstein and A.V. Olinto, *Ultra-High-Energy Cosmic Rays from Young Neutron Star Winds*, ApJ **533** (2000) L123 [astro-ph/9912240].

[5] J. Arons, *Magnetars in the Metagalaxy: An Origin for Ultra-High-Energy Cosmic Rays in the Nearby Universe*, ApJ **589** (2003) 871 [astro-ph/0208444].

[6] C. Guépin, B. Cerutti and K. Kotera, *Proton acceleration in pulsar magnetospheres*, A&A **635** (2020) A138 [1910.11387].

[7] H.E.S.S. Collaboration, A. Abramowski, F. Aharonian, F.A. Benkhali, A.G. Akhperjanian, E.O. Angüner et al., *Acceleration of petaelectronvolt protons in the Galactic Centre*, Nature **531** (2016) 476 [1603.07730].

[8] H. E. S. S. Collaboration, H. Abdalla, A. Abramowski, F. Aharonian, F. Ait Benkhali, A.G. Akhperjanian et al., *Characterising the VHE diffuse emission in the central 200 parsecs of our Galaxy with H.E.S.S.*, A&A **612** (2018) A9 [1706.04535].

[9] MAGIC Collaboration, V.A. Acciari, S. Ansoldi, L.A. Antonelli, A. Arbet Engels, D. Baack et al., *MAGIC observations of the diffuse γ-ray emission in the vicinity of the Galactic center*, A&A **642** (2020) A190 [2006.00623].

[10] F. Rogers, S. Zhang, K. Perez, M. Clavel and A. Taylor, *New Constraints on Cosmic Particle Populations at the Galactic Center Using X-Ray Observations of the Molecular Cloud Sagittarius B2*, ApJ **934** (2022) 19.

[11] F. Guo and W.G. Mathews, *The Fermi Bubbles. I. Possible Evidence for Recent AGN Jet Activity in the Galaxy*, ApJ **756** (2012) 181 [1103.0055].

[12] H.Y.K. Yang, M. Ruszkowski and E.G. Zweibel, *Fermi and eROSITA bubbles as relics of the past activity of the Galaxy's central black hole*, *Nature Astronomy* **6** (2022) 584.

[13] A. Marcowith, V.V. Dwarkadas, M. Renaud, V. Tatischeff and G. Giacinti, *Core-collapse supernovae as cosmic ray sources*, MNRAS **479** (2018) 4470 [1806.09700].

[14] G. Morlino, P. Blasi, E. Peretti and P. Cristofari, *Particle acceleration in winds of star clusters*, MNRAS **504** (2021) 6096 [2102.09217].

[15] IceCube Collaboration, *Observation of high-energy neutrinos from the Galactic plane*, *Science* **380** (2023) eaat1338.

[16] R. Bartels, S. Krishnamurthy and C. Weniger, *Strong Support for the Millisecond Pulsar Origin of the Galactic Center GeV Excess*, Phys. Rev. Lett. **116** (2016) 051102.

[17] M. Kachelrieß, I.V. Moskalenko and S. Ostapchenko, *AAfrag: Interpolation routines for Monte Carlo results on secondary production in proton-proton, proton-nucleus and nucleus-nucleus interactions*, *Computer Physics Communications* **245** (2019) 106846.

[18] S. Koldobskiy, M. Kachelrieß, A. Lskavyan, A. Neronov, S. Ostapchenko and D.V. Semikoz, *Energy spectra of secondaries in proton-proton interactions*, Phys. Rev. D **104** (2021) 123027 [2110.00496].

[19] M. Tsuboi, T. Handa and N. Ukita, *Dense Molecular Clouds in the Galactic Center Region. I. Observations and Data*, ApJS **120** (1999) 1.

[20] S. Molinari, J. Bally, A. Noriega-Crespo, M. Compiègne, J.P. Bernard, D. Paradis et al., *A 100 pc Elliptical and Twisted Ring of Cold and Dense Molecular Clouds Revealed by Herschel Around the Galactic Center*, ApJ **735** (2011) L33 [1105.5486].

[21] M. Tsuboi, K.-I. Tadaki, A. Miyazaki and T. Handa, *Sagittarius A Molecular Cloud Complex in $H^{13}CO^+$ and Thermal SiO Emission Lines*, PASJ **63** (2011) 763.

[22] C. Battersby, E. Keto, D. Walker, A. Barnes, D. Callanan, A. Ginsburg et al., *CMZoom: Survey Overview and First Data Release*, ApJS **249** (2020) 35 [2007.05023].

[23] GRAVITY Collaboration, R. Abuter, A. Amorim, M. Bauböck, J.P. Berger, H. Bonnet et al., *Improved GRAVITY astrometric accuracy from modeling optical aberrations*, A&A **647** (2021) A59 [2101.12098].

[24] D. Gaggero, A. Urbano, M. Valli and P. Ullio, *Gamma-ray sky points to radial gradients in cosmic-ray transport*, Phys. Rev. D **91** (2015) 083012 [1411.7623].

PoS(ICRC2023)1069